Genome-based analysis of head and neck cancers

PhD Thesis

Gombos Katalin MD

B-149 Molecular Epidemiology of Cancers Doctoral Program

Doctoral School of Clinical Medicine

Doctoral School leader: Dr. Kovács L. Gábor

Program leader and consultant: Dr. Ember István

Dr. Kiss István

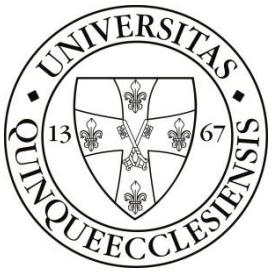

Pécs University

Faculty of Medicine 2016

I. Introduction

Head and neck region generally construed to comprise the base of skull and facial bones, sinuses, orbits, salivary glands, oral cavity, oropharynx, larynx, thyroid, facial and neck musculature and lymph nodes draining these areas, thereby tumors occurring in the region are very diverse according to location and histopathology as well as clinical symptoms and behaviour. Scientific literature and clinical practice maintained dual categorization for head and neck cancers. In proper, neoplasms of the middle ear, nasal cavity, nasal and perinasal sinuses, oral cavity, pharynx and larynx reckoned to this region. In wider sense tumors of the thyroid, parathyroid and salivary glands along with malignancies of the skin of this anatomical region belong to head and neck region cancer entities.

I.2. Development of cancers of the oral cavity, meso- and hypopharynx

Approximately 98% of head and neck cancers show sporadic occurrence and follow a multistep developmental process which is induced by environmental exposure. The most widely accepted hypothetic model for the tumor development is the *cancer field theory* also known as *tissue organization field theory*. Cancer field theory implicates that multiple genetic alterations (mutation, amplification, chromosome aberration) induced by summation of environmental exposures establish tumor initiation in basal cells of the squamous epithelium. Through cell division, daughter cells form a patch lesion. Contiguous clonal expansion result that the original genetically altered cell population mantle as a cancer field, which is not differ on the tissue phenotype from the normal mucosal surface. Cancer field subserve oral precursor lesion (OPL) development. Further genetic and epigenetic changes that turn out in OPL drive *in situ* and invasive cancer formation. Cancer field also promotes synchronous precursor lesion and second primary tumor emergence.

I.3. Development of thyroid tumors

Thyroid cancer originates from parafollicular cells (medullary) and follicular cells (non-medullary), which account for over 90% of all thyroid cancer cases. Around 70-80% of malignant neoplasms belong to papillary thyroid cancer (PTC) based on histological evaluation. PTC is associated with infiltrative growth, multicentric appearance and frequent lymph node metastasis. Histological hallmarks of follicular thyroid cancer (FTC) show many similarities to benignant follicular adenoma (FA). Biological behavior of these tumors is primarily influenced by presence or absence of capsular and vascular invasion. Presence of genetic mutations largely maintains the development of thyroid cancer subtypes with follicular cell origin and their histological transformation.

II. Objectives

II.1. miRNA pattern analysis in oral squamous cell carcinoma:

- construction of an oral squamous cell cancer (OSCC) specific marker panel of 12 selected miRNAs
- comparison of miRNA expression results with clinical and histological characteristics of the OSCCs and environmental, demographical and lifestyle etiological factors of the patients
- specification of cancer location, stage and grade associated miRNA expression patterns

II.2. target mRNA expression analysis of the miRNAs identified in OSCC

- confirmation of miRNA-mRNA regulatory modules which can functionally connect inflammation to carcinogenesis

II.3. miRNA expression analysis of meso- and hypopharynx squamous cell cancers

- miRNA expression pattern detection of the tumoral and peritumoral epithelium following a self-defined mapping biopsy strategy
- molecular modeling of the the tissue organization field by stepwise comparison of miRNA signature in peritumoral tissues

II.4. mRNA microarray analysis of thyroid tumors:

- high density microarray analysis of well differentiated early stage thyroid tumors with follicular cell origin (PTC, FTC, FA)
- selection of an mRNA marker set which can be available to supplement molecular differentiation of histological tumor types

II. Material and Methods

III.1. Sample collection

III.1.1 OSCC samples: forty OSCC samples were obtained from patients undergoing primary oral surgery for verified oral cancer at the Department of Oral and Maxillofacial Surgery at Dentistry, Oral and Maxillofacial Surgery Clinic in Pécs University. Sample collection was carried out only during R0 resections of I-II TNM stage OSCCs and biopsies were taken from the tumour tissues. For normal controls, biopsies were taken from the remote part of the reconstruction flaps.

III.1.2. Meso- and hypopharynx squamous cell cancer samples: were collected from patients diagnosed and treated at the Department of Otorhinolaryngology, Head and Neck Surgery of the Clinical Centre of Pécs University. Mapping biopsy sampling followed a standard strategy from the tumorous and peritumoral tissues, according to the following orders: tumor (0), peritumoral mucosal tissue at 1 cm distance from tumor margain (1), 2 cm distant mucosal tissue (2), normal mucosa from 3 cm distance (3). miRNA expression analysis enrolled 52 tissue samples from 13 patients (8 mesopharyngeal cancers and 5 tumors from the hypopharynx). Tumor tissue samples were clinico-pathologically classified into grade II, III and IV squamous cell carcinomas.

III.1.3. Thyroid tumor samples: were obtained from patients with benign and clinically early-stage malignant thyroid tumors (T1, N0, M0) undergoing surgery at the First Department of Surgery in Debrecen University. Histopathological classification was confirmed by an endocrine pathologist. Tumour samples of follicular adenoma (n=8), follicular carcinoma (n=7), papillary carcinoma (n=10) and normal thyroid tissue (from patients who underwent total thyroidectomy n=20) were selected for our investigations.

III.2. Laboratory analysis

III.2.1. RNA isolation from oral- mesopharyngeal and hypopharyngeal tissue samples: total cellular (tc)RNA was isolated with chemical extraction followed by solid phase extraction on silica columns provided by the High Pure miRNA isolation kits (Roche, Mannheim, Germany) according to the manufacturer's instructions. The quality of the yielded miRNA fraction was checked by spectrophotometry (MaestroNano, Maestrogen Inc., Hsinchu, Taiwan) and miRNA samples of higher than 1.9 optical density at 260/280 nm were used for further reverse transcription.

III.2.2. Reverse transcription: Samples were reverse transcribed in 5 µl reactions using the Universal cDNA synthesis kit (Quiagen, Woburn, MA, USA) with random hexamer priming. All tcRNA samples were corrected for 5 ng/µl concentrations in the RT mix. Reverse transcription reactions were carried out in Light Cycler glass capillaries (Roche) in a Light Cycler 2.0 thermocycler (Roche). Freshly synthesized cDNA chilled at 4˚C and immediately proceeded to PCR reactions. Quality control of cDNA was checked on 1% agarose gel electrophoresis.

III.2.3.Quantitatív real-time PCR: The PCR amplification was performed in a LightCycler® 480 Real-Time PCR System (Roche) in 96 well plates. Plate design contained two internal controls and an interplate calibrator for each investigated miRNA. MiCury human LNA™ PCR primer sets (Exiqon, Vedbaek, Denmark) were obtained as specific primers for hsa-miR-21, -155, -191, -146a, -221 and hsa-miR-222 and a set of miRNA specific primers with custom design: hsa-miR-21, -27a, -34a, -143, -146a, -148a, -155, -221, -223 (TIB MOLBIOL, Gyál, Hungary) for OSCC and hsa-miR-21, -27a, -34a, -143, -146a, -148a, -155, -221 (TIB MOLBIOL) for meso- and hypopharynx squamous cell samples. Plate layout design was maintained for triplicates of the samples according to each miRNA with two reference genes: hsa- 5S rRNS and U6 snRNS (Exiqon).

Target mRNA expression detection: Roche Ready-To-Use Custom Panel was used (Roche, Mannheim, Németország) representing tumor necrosis factor α interacting protein 1 *(Tnip1),* vascular cell adhesion molecule *(Vcam),* nuclear factor kappa B 1 and 2 (*Nfκb1, Nfκb2),* Toll-like receptor-1 (*Tlr1)* and inhibitor of κ light polypeptide gene enhancer in B-cells, kinase γ *(Iκbkg).* Reference genes were glyceraldehyde-3-phosphate dehidrogenase (*Gapdh)* and hypoxantine phosphoribosyltransferase *(Hprt1),* and positive control was *ß-actin.* Primer sequences were designed and downloaded from Universal Probe Libraryben (UPL/ roche-applied-science.com).

III.2.4. Microarray: experiments were completely carried out in the Functional Genomic Laboratory at Biology Research Center of the Hungarian Academy in Szeged. A total of 20,000 human gene-specific, aminomodified oligonucleotides were purchased (Sigma-Operon, Budapest, Hungary) and arrayed onto PXM oligonucleotide slides (Full Moon Biosystems, Sunnyvale, CA, USA). using a MicroGrid Total Array System (BioRobotics, Cambridge, UK) spotter. DNA elements were deposited in duplicate in distinct areas of the array in 300fmol/µl concentration. Two micrograms of total RNA were reverse transcribed using a poly-dT primed Genisphere Expression Array 900 PCR system (Genisphere, Hatfield, PA, USA) All the other probe preparation steps were carried out according to the manufacturer's instructions (Genisphere). Both the first step cDNA hybridization and the second step capture reagent (2.5 µl of each Cy5 and Cy3) hybridization were carried out in a Ventana hybridization station (Ventana Discovery, Tucson, AZ, USA) using the antibody protocol. After hybridization, the slides were washed in 0.2x salt sodium citrate then dried and scanned. Each array was scanned under a green (543 nm for Cy3 labeling) or a red laser (633 nm for Cy5 labeling) using a ScanArray Lite (GSI Lumonics, Billerica, MA, USA) scanning confocal fluorescence scanner. Scanned output files were analyzed using the GenePix Pro 5.0 software (Axon Instruments Inc., Foster City, CA, USA). For each channel, the median values of feature and local background pixel intensities were determined.

III.2.5. Statistical analysis: *In miRNA expression evaluation of oral, meso- and hypopharyngeal squamous cell cancer* Exor 4 LightCycler 480 software was used to determine the crossing point cycle (C_p) values. Outlier results with C_p standard deviation greater than 0.5 were excluded from further analysis. Both *U6* snRNA and the *5S* rRNA were tested as potential reference genes and *U6* snRNA was selected for normalization. miRNA expression values were normalized and calculated by using relative quantification with the 2^{-dCp} method as $\Delta C_p = C_p$ miR of interest $- C_p$ 5SrRNA. Relative miRNA expression results from the sample triplicates were averaged. Expression results were analyzed with two-tailed paired sample *t*-test, receiver operating characteristic (ROC) curve analysis, general linear model (GLM) and multivariate logistic regression analysis by SPSS version 21.0 (SPSS Inc., Chicago, IL, USA) and p values <0.05 were considered to be statistically significant. All graphs were also created by SPSS 21.0.

In case of the thyroid mRNA expression microarray background corrected expression data was filtered for flagged spots and weak signal and technical replicates on the same array were averaged. Normalization was performed using the print-tip LOWESS method. The one-sample t-test was used in order to determine the genes to be regarded as regulated. Expression ratios were log-transformed to fulfill the t-test's requirement for a normal distribution. Genes for which the mean of log-ratios across the biological replicates was equal to zero at a significance level ·=0.05 were considered to have an unchanged expression. On the other hand, genes having a p-value smaller than · and an average fold-change of the four data points of at least 2.0-fold were considered as modulated genes.

IV. Results

IV.1. miRNA pattern analysis of oral squamous cell carcinoma

1. experimental set

Relative quantification results of miRNA expression observed in OSCC samples and adjacent normal mucosal tissues is demonstrated in *Figure 1*.

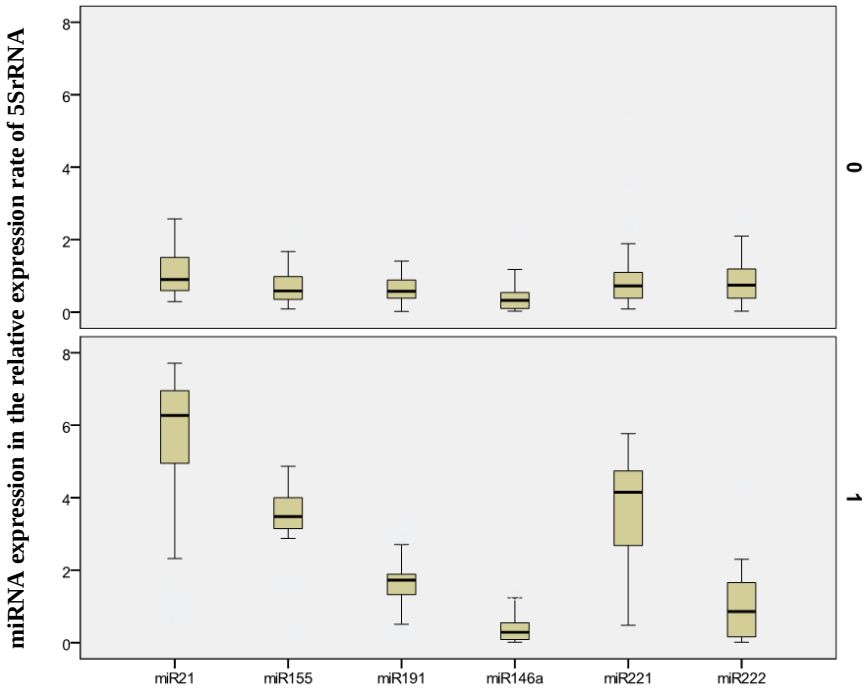

Figure 1: miRNA expressions oral squamous cell carcinoma (1) and autologous normal mucosa (0). Relative quantification values were calculated according to the second derivate maximum method and normalized to 5S rRNA expression.

All investigated miRNAs were over expressed in the OSCC samples compared to their expression in their adjacent normal tissues. The most abundantly expressed miRNAs were miR-21, miR-221 and miR-155 in the tumours and miR-146a was found to be expressed at very low amounts. The most characteristic difference and clearest segregation of OSCC versus normal controls by expression were found in the case of miR-155. Expression values of miR-21 and miR-221 exhibited 4 to 5 fold elevation in the OSCC samples compared to normal tissue, although there was a relatively higher scatter in their distribution. Lower elevation of expression was seen in the case of miR-191 and no observable difference was found for miR-222 and miR-146a.

Comparison of OSCC tumor samples with their autologous normal mucosal pair from the same patient paired sample t-test analysis revealed four of the analyzed miRNAs miR-21 (p=0,01), miR-155 (p=0,01), miR-191(p=0,03) and miR-221 (p=0,01) as having statistically significant expression changes in the tumors. During comparative analysis of miRNA

expression rates reflected to the total expression (*Figure 2.*) marked differences were observed according to tumor location.
ROC curve analysis is presented in *Figure 3*. Testing accuracy of the miR expressions is represented as the area under the curve which was found to be 90% for miR- 221 and higher than 90% in case of miR-21, miR-155 ($p \leq 0{,}05$).

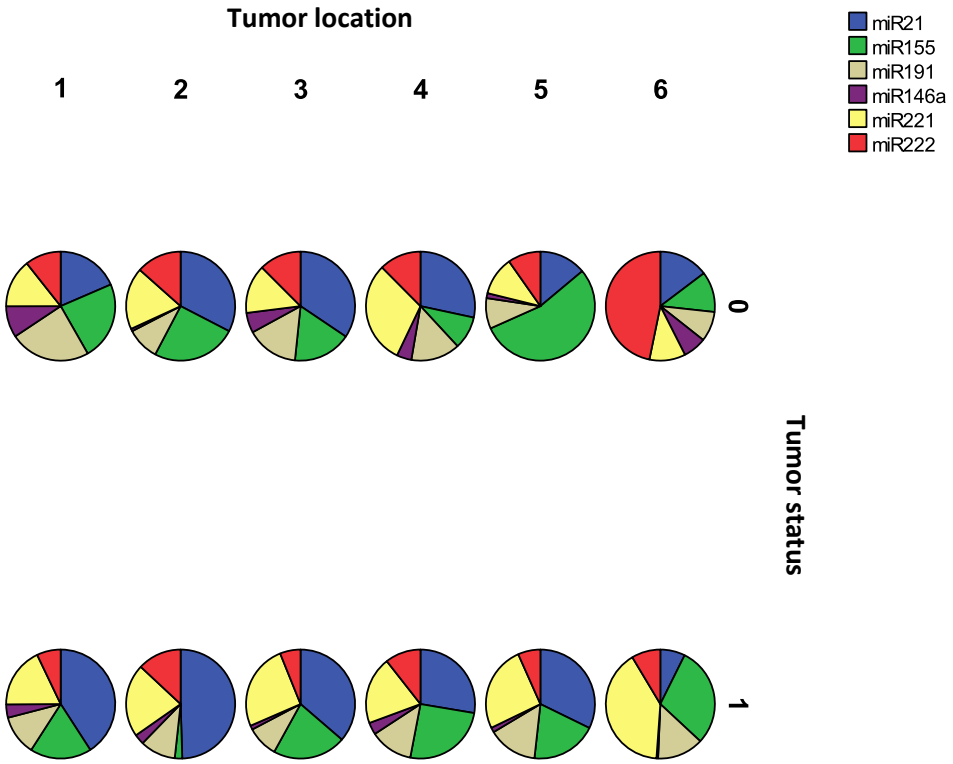

Figure 2: Differences of miRNA expressions calculated as proportion of the total expression in OSCC (1) and normal mucosa (0) according to tumor location (1: lip, 2: bucca, 3: tongue, 4: floor of the mouth, 5: gingiva, 6: palate)

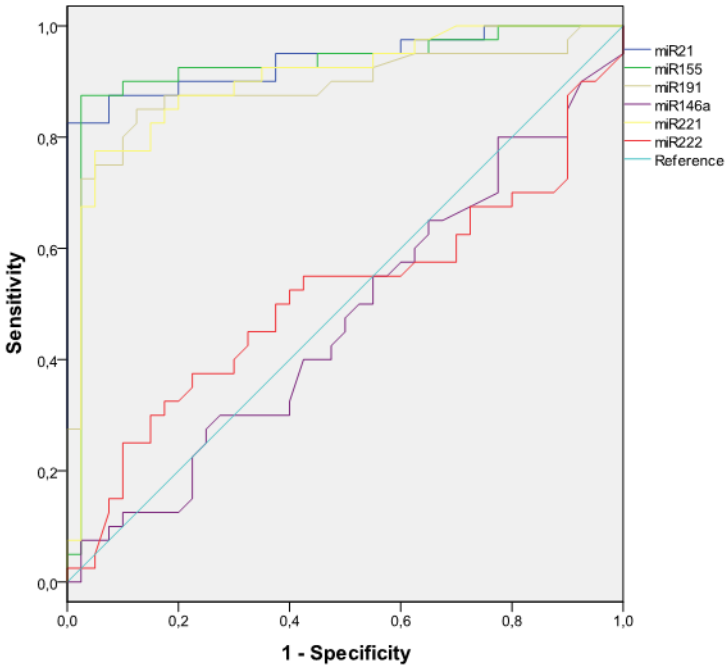

*Figure 3. :*Receiver operating characteristic curve analysis.

2. experimental set

OSCCs and autologous normal mucosal samples were evaluated on a larger set of custom designed primers. Due to the fact that we used 12 miRNA primer pairs instead of 6 we achieved more detailed patterns and correlation differences according to tumor site. Additionally we integrated matching epidemiological, demographical, clinical and pathological records with miRNA expression data and subjected to GLM and multivariate logistic regression analysis. Age, sex, tumor location, TNM classification, tumor grade, tumor size, lymph node metastasis and tumor recidive status were the independent factors in the analysis. MiRNA pattern changes were mostly related to tumor location, sex and age of the patient, tumor size, TNM stage and tumor grade. In GLM analysis miR34a (F=9,221), -143 (F=6,04), -196a (F=7,14) and -223 (F=11,96) expressions depended significantly from grade of the tumors, miR-155 level (F=5,7) was influenced by TNM class, miR-93 (F=3,67) was sensitive to tumor size and miR-205 (F=5,03) alteration correlated significantly to lymph node metastasis ($p \leq 0,05$).

IV.2. target mRNA expressions in OSCCs

Two-tailed paired sample t-test analysis confirmed significantly up-regulated expressions of vascular cell adhesion molecule (Vcam, p=0,050) and toll like receptor 1 (Tlr1, p=0,027) in tumor tissues compared to autologous normal mucosa samples. Tlr1 is one of the most effective activating receptorial mediator of NFκB signalling pathway while *Vcam* is a downstream target of *Nfκb1* in the cell survival regulatory network.

IV.3. MiRNA expression analysis of mapping biopsy samples from meso- and hypopharyngeal tissue samples

To achieve the miRNA expression pattern based cancer field detection we analyzed tumor tissue and microscopically intact mucosal tissue samples that were taken from definite distances from the tumor margin. We found sequential miRNA expression alterations moving away from the tumor margin towards the most distant mucosal areas at 3cm. (*Figure 4.*). On *t-test* evaluation tumor tissues and 1 cm distant peritumoral tissues only differed in miR-21 (p=0,01), -27a (p=0,01) and -221 (p=0,29) expression. Tumorous tissues and normal mucosa 2 cm away differed in miR-21 (p=0,01), -27a (p=0,01), -146a (p=0,03) and -155 (p=0,05) expressions, which were found to be overexpressed and miR-34a (p=0,023), -143 (p=0,01) that were significantly down regulated in the tumorous tissues. The largest change was seen during the comparison of tumors and the mucosa at 3cm range. All investigated miRNAs were significantly deregulated except miR-205.

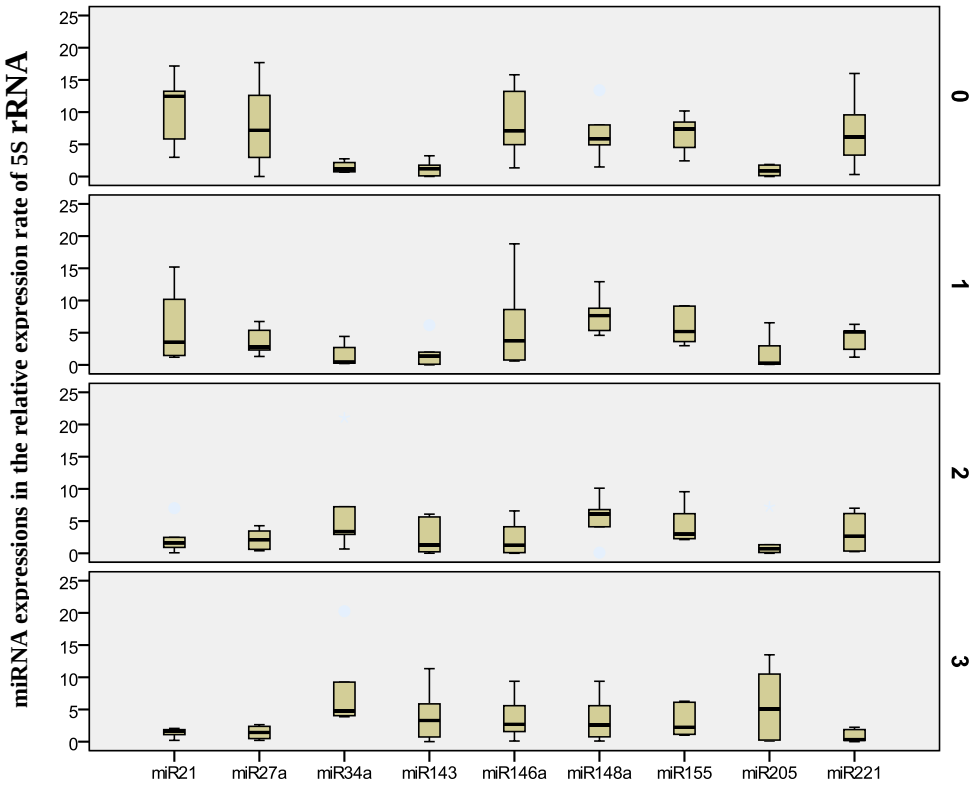

Figure 4: MiRNA expression changes in tumors and peritumoral tissues of meso- and hypopharynx squamous cell cancers. Expressions are calculated in relative quantification rate of 5S rRNA expression. (0) tumor, peritumoral normal tissues (1) 1 cm, (2) 2 cm, (3) 3cm from tumor margin.

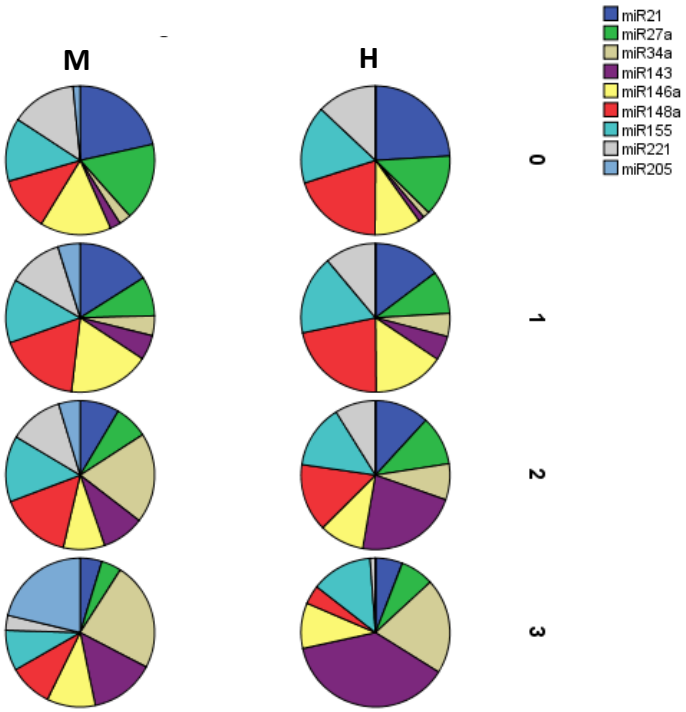

Figure 5: miRNA expresson rates reflected to total expression in meso-(M) and hypopharynx (H) squamous cell carcinoma and peritumoral tissues: (0) tumor, peritumoral normal tissues (1) 1 cm, (2) 2 cm, (3) 3cm from tumor margin.

Individual miRNA expressions calculated for overall expression reflected interesting pattern alterations. In cancer cells miR-21, miR-27a, miR-221 give neraly 50% of the cells' total miRNA expression. This number is barely 15% in cells localized in 3 cm distant normal mucosal tissues. miR-34a and miR-143 show exactly the opposite, their expression rates are below 10% in tumor tissue, and growing up step by step to 40% as we are going further from the tumor. Mucosal expressions observed 1 cm far from surgical excision's line shows little difference from those of the the tumors', while at the distances of 2 and 3 cm these rates differ prominently. Samples from 2 cm range have more common pattern features with intact mucosa in the distance of 3cm. Comparing the results of meso- and hypopharynx miRNA expression rates on multivariate logistic regression alterations of miR-21 (p=0,006), miR-143 (p=0,001), miR-155 (p=0,041). In samples from hypopharynx miR-21, 143 and 155 have shown significantly higher expression rates.

IV. 4. mRNA microarray analysis of thyroid tumors:

Significant expression differences of 258 genes, underexpression of 233 and overexpression of 25 genes, were found in the thyroid tumor samples of follicular adenoma, follicular carcinoma and papillary carcinoma compared to the normal thyroid tissue. Underexpressions were more expressed in all tumor samples than overexpressions and showed an increase in number in the malignant histiotypes (*Figure 6.*)

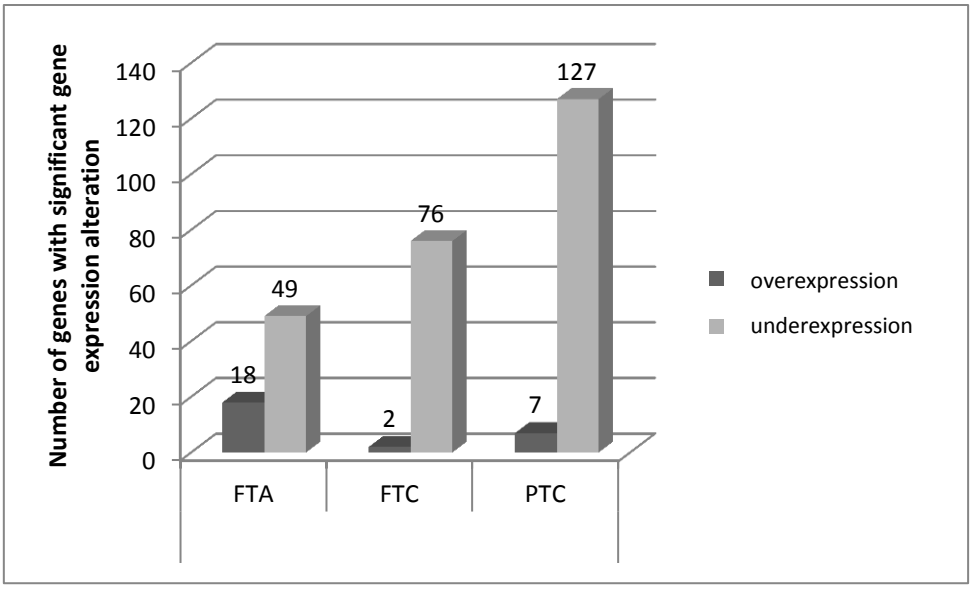

Figure 6: Number of significantly deregulated genes found in the different hystiotypes of thyroid tumors. FTA: follicular thyroid adenoma, FTC: follicular thyroid carcinoma, PTC: papillary thyroid carcinoma.

The underexpressed genes exhibited many overlaps between the tumour groups (Tables II and III). Moreover 25 out of 49 underexpressed genes found in follicular adenoma exhibited overlaps with the malignant histological types. Analysing these overlapping genes between the benign and malignant histiotypes, the underexpression of Bruton's tyrosine kinase (BTK), G protein coupled receptor 30 (GPR 30), apelin, E-cadherin (CDH9) and CDP-diacylglycerol (CDP-DAG) were identified in follicular adenoma and follicular carcinoma, while the underexpressed genes in follicular adenoma and papillary carcinoma included interleukin 12 receptor ,-2 (IL12R,-2) (Table II). Overlaps of underexpressions in the malignant histiotypes (follicular carcinoma and papillary carcinoma) involved phospholipase D1 (PLD1) and mitogen-activated protein kinase 10 (MAPK10). We also found some novel genes down-regulated in follicular and papillary thyroid carcinoma, which had not been reported yet in thyroid malignancies, such as SOX21 and NIL-2-A. However the consequent significant underexpression of three particular genes in all investigated tumour groups was remarkable: Peroxisome proliferator-activated receptorgamma (PPARγ), eosinophil-derived neurotoxin and urotensin II (Table III). We found small number of constitutively up-regulated genes in the investigated tumor histiotypes and this number showed further decrease in the malignant groups, whereas these up-regulated genes were characteristic to the different tumor histiotypes. The most considerable was the EDA1 overexpression identified in follicular thyroid adenoma and the cyclin D1 (CYLD1) overexpression represented in papillary carcinoma. Among the overexpressed genes just one was found to be significantly regulated in all follicular tumor types: NFκB.

ID	Name	log. rate	p value
	Follicular adenoma (FA)		
AB044385_1	Transmembrane molecule with thrombospondin module	2.225	0.001
AF152323_1	Protocadherin gamma A3	2.417	<0.05
AF387908_1	MHC class I antigen	2.087	0.010
BC000814_1	TG-interacting factor (tale family homeobox)	2.263	<0.05
BC003382_1	Sorting nexin 2	2.166	0.006
BC011027_1	Ectodysplasin A isoform 1 EDA1	2.285	0.001
NM031942_1	Cell division cycle associated protein 7 isoform 1	2.167	0.009
NM080798_1	Alpha 1 type XIII collagen isoform 2	2.460	<0.05
XM012425_1	Lysyl oxidase-like 1	2.196	<0.05
XM030577_1	Potential phospholipid-transporting ATPase Iia	2.203	0.001
XM051590_1	Nuclear pore protein GP210 precursor	2.004	<0.05
	Follicular adenoma (FA)/ Follicular carcinoma (FTC)		
XM166349_1	Nuclear factor of kappa light polypeptide gene enhancer in B-cells, NFKB	3.426/2.066	0.021/0.007
	Follicular carcinoma (FTC)		
XM170650_1	Riken cDNA 4921522e24	2.237	0.016
	Papillary carcinoma (PTC)		
AB083586_1	Putative G-protein coupled receptor	2.576	<0.05
AJ250014_1	Cyclin D1, CYLD1	2.235	<0.05
BC015753_1	GRO2 oncogene	2.088	<0.05
D89501_1	Salivary proline rich protein P-B, PB1	2.279	0.023
K03208_1	Proline rich protein BstNI subfamily, PRB2	2.166	0.001

Table I.: Significantly overexpressed genes in the different types of thyroid tumors

ID	Name	log. rate	p value	log. rate	p value
		FTA		**FTC**	
AF153762_1	Bruton's tyrosine kinase, BTK	-2.025	0.0075	-2.661	0.0140
AF208694_1	Impact	-2.594	0.0013	-2.689	0.0001
BC011634_1	G protein-coupled receptor 30, GPR30	-3.429	0.0004	-2.138	0.0420
BC021104_1	Apelin	-2.024	0.0011	-2.162	0.0280
M55513_1	Potassium channel protein	-2.396	0.0001	-3.810	0.0007
NM_016279_1	E-cadherin	-2.197	0.0001	-2.048	0.0416
NM_145752_1	CDP-diacylglycerol–inositol 3-phosphatidyl-transferase isoform 2	-3.327	0.0002	-2.854	0.0001
		FTA		**PTC**	
BC002530_1	ADP-ribosylation factor-like 2, ARL2	-2.016	<0,05	-2.525	0.0086
NM_000946_1	Primase, polypeptide 1 (49kd); PRIM1	-2.160	<0,05	-3.368	0.0004
NM_001559_1	Interleukin 12 receptor, beta 2,IL12RB2	-3.000	<0,05	-2.593	0.0087
NM_002076_1	Glucosamine (N-acetyl)-6-sulfatase precursor	-2.567	<0,05	-3.140	0.0003
NM_006298_1	Zinc finger protein 192, ZNF192	-2.003	<0,05	-2.037	0.0411
NM_006484_1	Dual-specificity tyrosine-(y)-phosphorylation regulated kinase 1b isoform c	-2.050	<0,05	-2.870	0.0008
XM_007868_1	Sodium/hydrogen exchanger 5 (Na(+)/H(+) exchanger 5), NHE-5	-2.655	<0,05	-2.644	0.0071
		FTC		**PTC**	
AF052510_1	Phosphocholine cytidylyltransferase b	-2.562	0.0001	-2.123	0.0156
AF107044_1	DNA-binding protein,SOX21	-2.488	0.0010	-2.876	0.0075
AK091478_1	NIL-2-a zinc finger protein	-2.260	0.0004	-2.090	0.0051
NM_002662_1	Phospholipase d1, phophatidylcholine-specific; PLD1	-2.001	0.0001	-2.742	0.0005
NM_002753_1	Mitogen-activated protein kinase 10, isoform 1; MAPK10	-2.277	0.0002	-2.214	0.0092
NM_003691_1	Serine/threonine kinase 16, STK16	-2.250	0.0010	-3.074	0.0033
NM_005251_1	Forkhead box C2, FOXC2	-2.351	0.0012	-3.124	0.0001

Table II. Genes overlapping in underexpression FTA: follicular thyroid adenoma, FTC: follicular thyroid carcinoma, PTC: papillary thyroid carcinoma.

		FTA		FTC		PTC	
ID	**Name**	**log. rate**	**p value**	**log. rate**	**p value**	**log. rate**	**p value**
AF140630_1	Urotensin-II	-2.264	0.004	-4.106	0.001	-2.46	0.001
AF294009_1	Eosinophil-derived neurotoxin, RNS2	-2.113	0.024	-2.872	0.001	-2.501	0.014
AF308819_1	Nuclear receptor-interacting factor, PPARG	-2.647	0.001	-2.418	0.029	-2.371	0.001

Table III. Genes overlapping in underexpression FTA: follicular thyroid adenoma, FTC: follicular thyroid carcinoma, PTC: papillary thyroid carcinoma.

V. Discussion

V.1 Discussion of oral, meso- and hypopharyngeal squamous cell cancer miRNA pattern analysis

The carcinogenesis of oral-, meso- and hypopharyngeal squamous cell carcinomas are often described in the literature by the cancer field theory. The hypothesis can explain aggressive clinical features of these tumors such as rapid progression, high recidive rates, occurence of second primary tumors at a notably high rate. Although it could have many practical projections, molecular detection of the cancer field has not been modeled so far. miRNAs are defined by individual genetics, but they also play an important role as morphostatic factors on epigenetic level and they have been proven to be promising in the molecular characterization of numerous type of cancers. Taking advantage of the RNase resistency and stability of these small molecules that results high experimental reproducibility, we identified and visualized the cancer fields, which clearly showed correlation to the changes in the miRNA expression patterns. Some of the investigated miRNA markers: miR-21, -34a, -155 and -221 was found statistically significant in nearly every comparison. Previous studies have already indicated their role in the modified regulation of p53 in squamous cell carcinoma cell lines. Pattern of loss of expression of miR-34a and miR-143, which ate identified tumor suppressors by independent studies, was strongly associated with the tumorous phenotype according to our findings. MiR-146a and miR-148a are effective blockers of promoter specific repressors, which play a key role in NFκB antiapoptotic signaling pathway. These miRNAs play an important role at those signaling points which are shared by both the inflammatory and carcinogenetic pathways. Our subsequent target mRNA analysis confirmed their effect on NFκB linked gene expressions.

Analyzing miRNA expression rate patterns was an efficient method to distinguish the different tumor locations and tumor surrounding mucosal tissues. Using a well selected set of molecular markers can help us in the characterization of the peritumoral tissues on molecular level. Based on miRNA profile analysis the cancer field can be detected and postoperative recidive risk can be predicted.

V.2. Discussion of microarray analysis on thyroid tumors

Microarray analysis enables us to take a genome-wide cross-sectional snapshot of tumors. Analysis and comparison of these molecular snapshots makes it possible to identify characteristic steps of deregulation and dedifferentiation in tumorigenesis. Based upon these findings we can conclude that apart from limited number of heterogenous genetic alterations leading to the formation of thyroid tumors, this group of tumor can be characterized by consistent and specific molecular changes and behaved as a homogenous group in terms of gene expression. All the histiotypes of tumors investigated here contained significantly modulated genes acting on the NF-κB regulatory pathway (Figure 7).

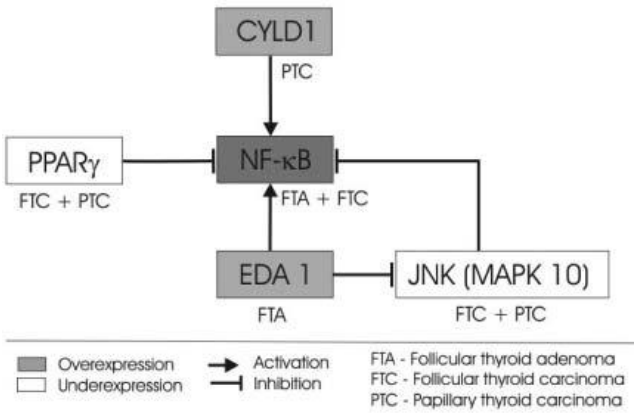

Figure 7. Gene interactions of NF-κB found in thyroid tumours.

We were thus able to define a key regulatory gene network that play essential role in early stage tissue architecture and cell survival maintenance of thyroid cancers with follicular origin. In follicular tumor variants (follicular adenoma and follicular carcinoma) NF-κB was found to be up-regulated. Follicular thyroid adenomas exhibited the overexpression of EDA1, which has a regulatory role in NF-κB-promoted transcription and JNK signaling. Malignant phenotypes (follicular thyroid carcinoma and papillary thyroid carcinoma) additionally represented constitutive down-regulation of genes (PPARγ and MAPK10/JNK) partaking in NF-κB inhibition. Furthermore in papillary thyroid carcinoma another regulatory gene (CYLD1) was consequently up-regulated, which is closely connected to NF-κB signaling. Our findings support that modulation of NF-κB signal transduction plays a crucial role in early thyroid carcinogenesis. Considering the fact that NF-κB has already been found to be a possible therapeutic target, our investigation could provide new possibilities for diagnostic, and preventative perspectives.

Summary of new results

1. miRNA expression analysis of early stage OSCC:
   a. We identified significant expression alterations according to miR-21, -27a, -34a, -93, -143, 146a, 148a, -155, -191, -196a, -203, -205, -221 and 223. Except miR-34a and -143, which were found to be down-regulated, all miRNAs showed overexpression in the cancer tissues. Through evaluation of biomarker test efficiency miR-21, -27a, -155, -191, -205, -221, -223 were proved to be specific and sensitive enough to distinguish tumorous tissues from normal mucosa.
   b. Using GLM analysis for the comparison of demographical and clinical factors with miRNA expression patterns we observed significant correlations of miR-34a, -143, -196a, -223 expression changes with histological grade, miR-155 alteration associated to TNM stage, miR-93 with tumor size and miR-205 influenced by lymph node metastasis development.
   c. Taken in consideration all types of statistical evaluations we found miR-155 to be the most specific and sensitive marker for OSCC, reflecting the tumorous features and indicating TNM stage dependably.
2. Expression analysis of target mRNA molecules, which were functionally linked to NFκB signal transduction confirmed significantly deregulated mRNA transcripts.
   a. The NFκB focused panel showed significantly elevated *Vcam* and *Tlr1* mRNA levels in the OSCC samples and we also noticed a constitutive elevation of NfκB1 mRNA itself, but it did not reach statistical significance. OSCC samples showed synchronous changes in miRNA and target mRNA expression alterations, which observation underlines miRNA-mRNA modular effect.
3. We were able to demonstrate cancer field detection by miRNA expression profiles of meso- and hypopharynx squamous cell cancers and peritumoral tissues.
   a. By comparative miRNA expression analysis of tumorous and peritumoral normal tissues that were collected from definite distances away from the tumors we found stepwise sequential changes in miRNA levels. Cancer tissues showed correlation with miR-21, -27a and -221 elevations while peritumoral tissues expressed miR-21, -27a, -146a, and -155 dependently from the distance of the tumor margain. The ulterior mucosal range had significantly higher miR-34a and -143 expression values.
   b. Identification of site-specific miRNA in meso- and hypopharingeal cancers: miR-221 was specific for mesopharyngeal location and miR-148a for hypopharynx carcinomas. Relative quantity of miR-21, -143 and -155 were found all to be significantly higher in amount in hypopharynx tumors.
4. Early stage FTA, FTC and PTC evaluation on high density mRNA microarray demonstrated the possibility of molecular characterization by expression analysis.
   a. Significantly up- and downregulated genes were identified according to tumor histological type. Number of significantly underexpressed genes showed linear correlation with grade of malignity. Genes that were found to be overexpressed were specific for the different tumor type in which it was found, except NFκB. On combined analysis we recognized overlapping gene deregulations between the different tumor entities.
   b. We worked out a functional regulatory model for the overlapping genes that were found to have significantly altered regulation. NFκB was recognized to be the key regulator enrolling PPARγ, CYLD1, EDA and JNK as a network for apoptotic and tissue architecture regulation.

Aknowledgements

I'm very grateful to everybody who supported me in any way to carry out my thesis work. Especially I'd like to owe my thanks to:

- my consulent and program leader, Dr. Istvan Ember, who established scientific intellectual and infrastructural background for my everyday work. During the years we could spend together he had the greatest inspiration on my research interests
- my current supervisor Dr. Istvan Kiss for his professional support and guidance
- Dr. Lajos Olasz, leader of the Department of Oral and Maxillofacial Surgery, for the unmatchable cooperation on molecular epidemiological analysis of oral cavity tumors for so many years
- Dr. Imre Gerlinger, head of the Otorhinolaryngology, Head- and Neck Surgery Clinic, Dr. István Szanyi, associate professor, and Dr. Éva Orosz for their professional support and participation in all of my studies
- all members of our work group of Molecular Genomics in the Department of Public Health, who throughout the years gifted me with their unselfish help and support day by day: Dr. Katalin Gőcze, Dr. Eszter Szele, Dr. Krisztina Juhász, Zsuzsa Brunnerné Bayer, Mónika Herczeg and whom I can be the most thankful: Ágnes Szántódiné Molnár, who helped me the technical edition of all of my publications and the current thesis work
- to the National Excellence Program for their financial support I was granted through ACSJ Scholarship.

I would like to express my wholehearted thanks to my family for their loving support unwavering trust and patience gave me possibility to complete my work on the thesis.

Publications related to the thesis

1. **K Gombos**, E Szele, I Kiss, T Varjas, L Puskás, L Kozma, F Juhász, E Kovács, I Szanyi, I Ember
   Characterization of microarray gene expression profiles of early stage thyroid tumours.
   Cancer Genomics & Proteomics 406) pp. 403-409. (2007)

2. Gy Gőbel, **K Gombos**, E Szele, E Kálmán, F Budán, I Gerlinger, F Fiscina, I Szanyi, Á Ember, Á Németh, I Ember
   Retrospective analysis of malignant salivary gland tumor sin Hungarian population between 1987-2006.
   European Journal of Oncology 1404) pp. 209-215. (2009)

3. Gőcze K, **Gombos K**, Juhász K, Ember
   Környezeti karcinogének korai hatásainak mikro-RNS-alapú molekuláris epidemiológiai biomarkerekkel történő monitorizálása (új utak a primer prevencióban)
   Magyar Epidemiológia 802) pp. 83-95. (2011)

4. Gőcze Katalin, **Gombos Katalin**, Pajkos Gábor, Magda Ingrid, Ember Ágoston, Juhász Krisztina, Patczai Balázs, Ember István
   Mikro-RNS-ek jelentősége a molekuláris epidemiológiában.
   Orvosi Hetilap 152016) pp. 633-641. (2011)

5. Gobel G, Szanyi I, Revesz P, Bauer M, Gerlinger I, Nemeth A, Ember I, Gocze K, **Gombos K**
   Expression of NFkB1, GADD45A and JNK1 in Salivary Gland Carcinomas of Different Histotypes.
   Cancer Genomics & Proteomics 1002) pp. 81-87. (2013

6. **Gombos K**, Horvath R, Szele E, Juhasz K, Gocze K, Somlai K, Pajkos G, Ember I, Olasz L
   miRNA Expression Profiles of Oral Squamous Cell Carcinomas.
   Anticancer Research 3304) pp. 1511-1517. (2013)

7. Orosz E, **Gombos K**, Revesz P, Kiss I, Pytel J, Gerlinger I, Szanyi I
   Mikro-RNS-expressziós mintázatok mesopharynx-hypopharynx laphámcarcinomákban.
   Orvosi Hetilap 155027) pp. 1063-1070. (2014)

8. Rideg O, **Gombos K**, Miseta A, Kovács L G
   A humán papillómavírus nem válogat.
   Ime: Informatika és Menedzsment az Egészségügyben 1308) pp. 58-62. (2014)

Book chapter related to the thesis

Gombos K, Ember I

Molekuláris Közegészségtan.

In: Ember István, Kiss István, Cseh Károly (szerk.)
Dialóg Campus Tankönyvek – Natura Delectans sorozat, Budapest; Pécs: Pécsi Tudományegyetem Általános Orvostudományi Kar, 2013. pp. 99-106.